XRD and HREM Studies of Epitaxially Stabilized Hexagonal Orthoferrites $RFeO_3$ (R = Eu−Lu)

Alexei A. Bossak,*[†,‡] Igor E. Graboy,[†] Oleg Yu. Gorbenko,[†] Andrey R. Kaul,[†]
Maria S. Kartavtseva,[†] Vassily L. Svetchnikov,[§] and Henny W. Zandbergen[§]

Department of Chemistry, Moscow State University, 119899 Moscow, Russia, European Synchrotron Research Facility, B.P. 220 F-38043 Grenoble Cedex, France, and National Centre for HREM, Laboratory of Materials Science, Delft University of Technology, Rotterdamseweg 137, 2628 AL Delft, Netherlands

Received December 22, 2003. Revised Manuscript Received February 26, 2004

The formation of previously unknown hexagonal modifications of orthoferrites $RFeO_3$ (R = Eu−Lu) was observed on $ZrO_2(Y_2O_3)$ (111) substrates at 900 °C. XRD and HREM studies reveal epitaxial growth of the hexagonal film. The structure of the hexagonal $RFeO_3$ was assigned to the ferroelectric space group $P6_3cm$. The typical structural defects in the hexagonal $RMnO_3$ films on $ZrO_2(Y_2O_3)$ (111) are described. Parallel deposition on perovskite substrates results in the stable perovskite phase. The epitaxial stabilization concept successfully explains the experimental results.

Introduction

$RFeO_3$ compounds, where R is a trivalent rare earth cation, possess a perovskite structure (space group *Pnma*) for all rare earth cations. In contrast, a stable hexagonal $LuMnO_3$-type structure (space group $P6_3cm$) has been found for $RMnO_3$ compounds in the case of R of small ionic radius (Ho−Lu, Y, Sc). This structure can be described as dense oxygen-ion packing (ABCACB) with Mn^{3+} ions having coordination number CN = 5 (5-fold trigonal bipyramidal coordination), and R^{3+} with CN = 7 (7-fold monocapped octahedral coordination).[1]

In principle, there are no crystallographic limitations for the existence of hexagonal orthoferrites and the compounds with trigonal bipyramidal coordination of Fe^{3+} are known (i.e., $ErFeMnO_4$, $YbFeMnO_4$,[2,3] $LuFeCoO_4$, and $LuFe_2O_4$[4]). Also Shannon ionic radii of Mn^{3+} and Fe^{3+} are nearly the same (0.645 Å for CN = 6 and 0.58 Å for CN = 5).[5,6] Nevertheless, there are no reports in the literature on hexagonal orthoferrites in the bulk state. The hexagonal polymorphs of $RFeO_3$ were only synthesized as nanoparticles for R = Eu and Yb.[7] The result means that the free energy difference between perovskite and layered hexagonal polymorphs is still rather small for orthoferrites, similar to orthomanganites, and can be overbalanced by the contribution of the surface energy.

As we have demonstrated before, the unstable-in-bulk hexagonal $RMnO_3$ phase was obtained instead of stable perovskite polymorph due to the epitaxy on the proper substrates.[8,9] We will show here that the way is suitable for the synthesis of unstable-in-bulk hexagonal orthoferrites as well. Here we present the results of the XRD and HREM studies of the epitaxially stabilized hexagonal $RFeO_3$ films.

Experimental Section

Thin Films Preparation. The deposition runs were performed using a single-source MOCVD process. The new type of feeding system was proposed in the current work to provide a highly uniform low deposition rate. The principle of feeding was as follows. The porous pellet containing a mixture of the solid volatile precursors was extruded by a screw-gear against the high-speed abrasive disk. The powder shorn off the pellet was transported to a vertical evaporator by the argon flow. The uniform feeding rate as low as 10 mg/h can be easily reached with the device (Figure 1). For film deposition in solvent-free conditions such a system is preferable to a vibration feeder.[10]

The deposition temperature was 900 °C, the precursor evaporator temperature was 250 °C, the oxygen partial pressure was 0.33 kPa, and the total gas pressure was 0.67 kPa (the deposition rate was about 5 nm/min). $Fe(thd)_3$ and $R(thd)_3$, where thd = 2,2,6,6-tetramethylheptane-3,5-dionate, were used as precursors. The precursors were sublimed in a vacuum before being used in the MOCVD process. Deposition of films with the thickness 60−70 nm was performed simultaneously on (111) $ZrO_2(Y_2O_3)$ and (001) $SrTiO_3$ substrates.

(111) $ZrO_2(Y_2O_3)$ substrate has an excellent coincidence of oxygen crystallographic positions at the interface with the

---

* To whom correspondence should be addressed. Tel: +33 (0)4 76 88 22 97. Fax: +33 (0)4 76 88 29 04. E-mail: bossak@esrf.fr.

[†] Moscow State University.

[‡] European Synchrotron Research Facility.

[§] Delft University of Technology.

(1) Yakel, H. L.; Koehler, W. C.; Bertaud, E. F.; Forrat E. F. *Acta Crystallogr.* **1963**, *16*, 957.

(2) Nespolo, M.; Isobe, M.; Iida, J.; Kimizuka N. *J. Alloys Compd.* **2000**, *313*, 59.

(3) Nespolo, M.; Isobe, M.; Iida, J.; Kimizuka, N. *Acta Crystallogr. B* **2000**, *56*, 805.

(4) Isobe, M.; Kimizuka, N.; Iida, J.; Takekawa, S. *Acta Crystallogr. C* **1990**, *C46*, 1917.

(5) Shannon, R. D.; Prewitt, C. T. *Acta Crystallogr. B* **1969**, *25*, 925.

(6) Shannon, R. D. *Acta Crystallogr. A* **1976**, *32*, 751.

(7) Mizoguchi, Y.; Onodera, H.; Yamauchi, H.; Kagawa, M.; Syono, Y.; Hirai, T. *Mater. Sci. Eng.* **1996**, *A217/218*, 164.

(8) Bosak, A. A.; Dubourdieu, C.; Sénateur, J.-P.; Gorbenko, O. Yu.; Kaul, A. R. *Cryst. Eng.* **2002**, *5*, 355.

(9) Graboy, I. E.; Bosak, A. A.; Gorbenko, O. Yu.; Kaul, A. R.; Dubourdieu, C.; Senateur, J.-P.; Svetchnikov, V. L.; Zandbergen, H. W. *Chem. Mater.* **2003**, *15*, 2632.

(10) Samoylenkov, S. V.; Gorbenko, O. Y.; Graboy, I. E.; Kaul, A. R.; Tretyakov, Y. D. *J. Mater. Chem.* **1996**, *6*, 623.

10.1021/cm0353660 CCC: $27.50

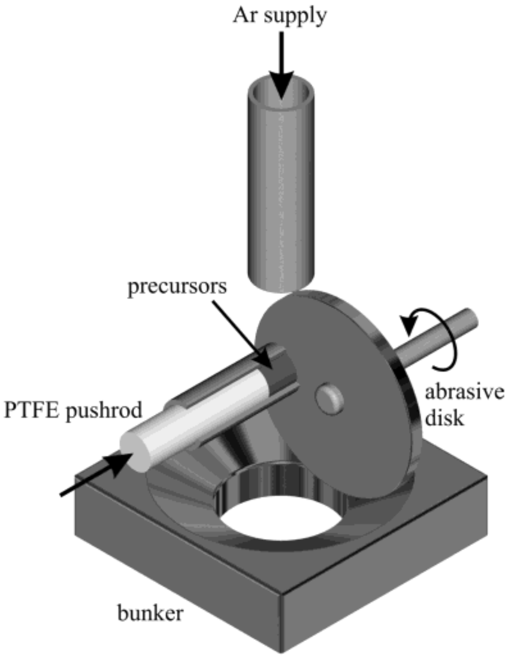

Figure 1. Sketch of the "shaving" feeder for the MOCVD system.

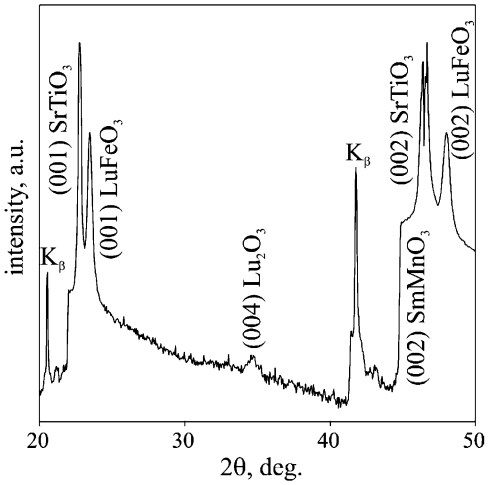

Figure 2. $\theta/2\theta$ Scan for the off-stoichiometric $LuFeO_3$ film deposited on (001) $SrTiO_3$; the Lu_2O_3 secondary phase reflection is visible.

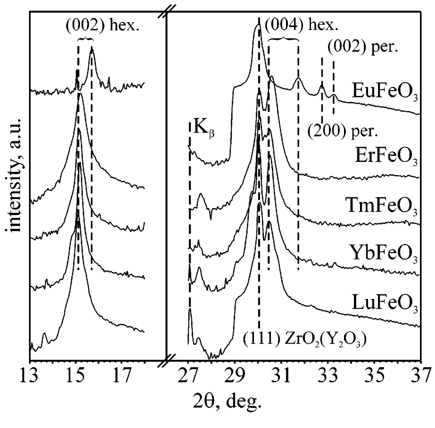

Figure 3. θ-2θ XRD patterns for $RFeO_3$ films on (111) ZrO_2-(Y_2O_3).

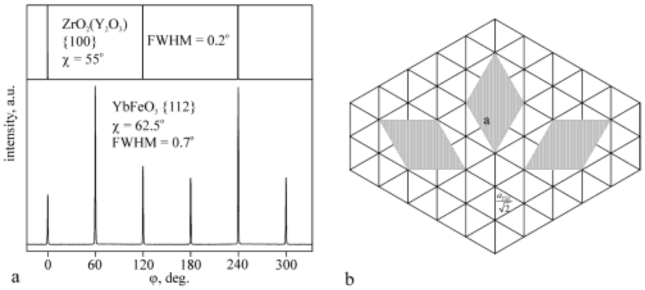

Figure 4. (a) φ-scans for (111) $ZrO_2(Y_2O_3)$ substrate and *c*-oriented hexagonal $YbFeO_3$ film; (b) the scheme of epitaxy.

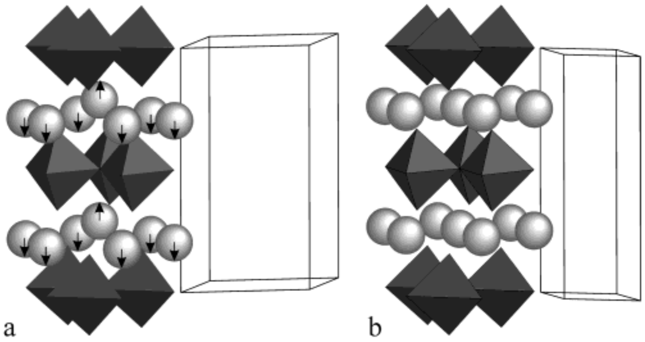

Figure 5. Models of the hexagonal $LuMnO_3$-type (a) and $YAlO_3$-type (b) structures. Decrease of Goldschmidt tolerance factor promotes the lowering of symmetry.

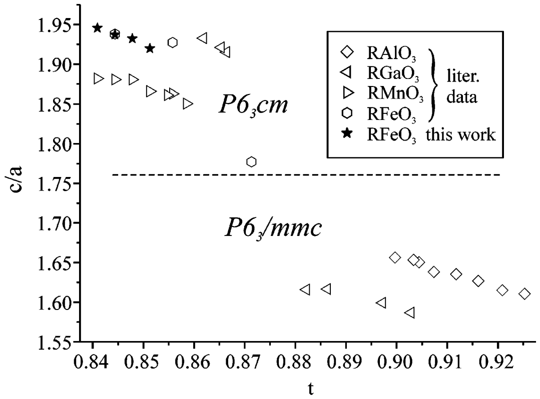

Figure 6. Hexagonal cell axis ratio as a function of Goldschmidt tolerance factor.

hexagonal $LuMnO_3$-type structure, and because of the proximity of Mn^{3+} and Fe^{3+} ionic radii the lattice parameters of the hexagonal $RFeO_3$ should be sufficiently close to those of substrate, as for $RMnO_3$. In principle, (111) MgO substrate can be suitable also (low mismatch), but the coincidence of oxygen positions is worse. The series of depositions was started from the heaviest rare earths, as we have expected the lowering of the free energy difference of the polymorphs with lowering of the ionic radius of R^{3+}.

Characterization Methods. The films were characterized by X-ray diffraction (XRD) using a DRON-3M two-circle diffractometer and a Siemens D5000 four-circle diffractometer (equipped with secondary graphite monochromator), and by high-resolution electron microscopy (HREM). Cross-sections of ion-milled film samples were studied using a Philips CM30UT microscope with a field emission gun operated at 300 kV. Electron diffraction patterns were recorded with a 1024 × 1024 pixel Photometrix CCD camera with a dynamic range of 12 bits. Electron diffraction (ED) was performed with spot sizes of about 10 nm, using a 15-μm condenser lens aperture. Exposure times ranged from 0.5 to 2 s.

Results and Discussion

$RFeO_3$ films on $SrTiO_3$ are epitaxial and consist of the perovskite phase only. In the pseudocubic notations

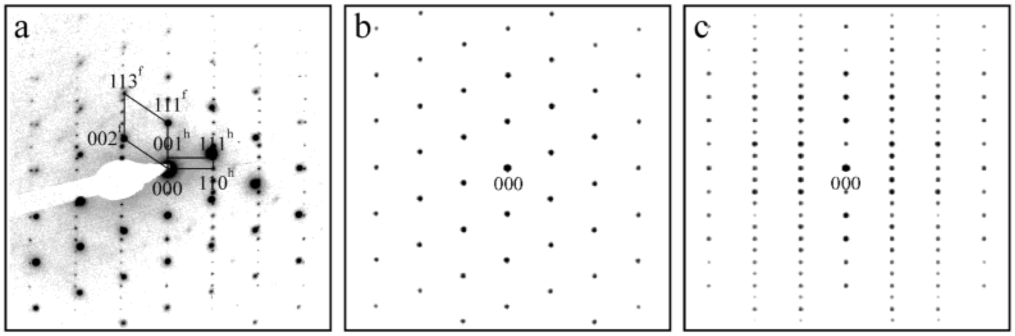

Figure 7. $(1\bar{1}0)$ zone diffraction pattern of $TmFeO_3$ film on $ZrO_2(Y_2O_3)$ (111) (a); ED model (b) and (c). Superscript *f* corresponds to the fluorite substrate and *h* corresponds to the hexagonal phase.

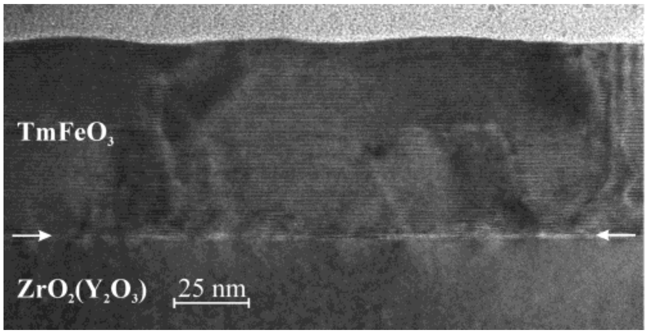

Figure 8. $(1\bar{1}0)$ Zone general view of hexagonal $TmFeO_3$ film on $ZrO_2(Y_2O_3)$ (111).

Table 1. Lattice Parameters of Hexagonal $RFeO_3$ Thin Films on $ZrO_2(Y_2O_3)$ (111) Substrates

R	*a*, Å	*c*, Å
Eu		11.27(2)
Er	6.09(1)	11.69(1)
Tm	6.02(1)	11.73(1)
Yb	6.03(1)	11.68(1)
Lu	6.04(1)	11.75(1)

Table 2. Atomic Coordinates Used in ED Modeling for $TmFeO_3$ and $ZrO_2(Y_2O_3)$

$TmFeO_3$	$P6_3cm$			$ZrO_2(Y_2O_3)$	$Fm3m$		
Tm (1)	0	0	0.2705	Zr(Y)	0	0	0
Tm (2)	1/3	2/3	0.2266	O	1/4	1/4	1/4
Fe	0.3212	0	0				
O(1)	0.3071	0	0.1699				
O(2)	0.6328	0	0.3397				
O(3)	0	0	0.4836				
O(4)	1/3	2/3	0.0189				

the relations of epitaxy are as follows ("cube-on-cube" growth):

$$(001)\ RFeO_3//(001)\ SrTiO_3;\quad [100]\ RFeO_3//[100]\ SrTiO_3$$

$\theta/2\theta$ scans reveal also the oriented impurities of cubic R_2O_3 (Figure 2) where R/Mn > 1, which was used for the fine composition adjustment besides EDX analysis.

XRD patterns of $LuFeO_3$, $YbFeO_3$, $TmFeO_3$, $ErFeO_3$, and $EuFeO_3$ deposited on (111) $ZrO_2(Y_2O_3)$ reveal reflections typical of a hexagonal $LuMnO_3$-type structure (Figure 3). The fingerprint of hexagonal phase is (002) reflection well-separated from the reflections of the perovskite polymorph. The hexagonal phase is *c*-oriented, which was confirmed by φ-scans and pole figures (Figure 4). Epitaxial relations were established as follows:

$$(001)_{\text{hex.}}\ RFeO_3//(111)\ ZrO_2(Y_2O_3);\quad \langle 1\bar{1}0\rangle_{\text{hex.}}\ RFeO_3//\langle 1\bar{1}0\rangle\ ZrO_2(Y_2O_3)$$

The parameter *a* was calculated from reflections measured by off-plane $\theta/2\theta$ scans, except for $EuFeO_3$ because of the low hexagonal phase content. The in-plane lattice mismatch in the Er−Lu series is relatively high (3−4.5%) so the measured parameters should conform to the relaxed epitaxial strain. The lattice parameters of the films are given in Table 1.

The *c* parameter of the $EuFeO_3$ film is much smaller than that which follows from the extrapolation of the parameter as a function of the ionic radius for other $RFeO_3$ phases, which can be explained by important strain contribution. The latter is due to the very small thickness of the hexagonal $EuFeO_3$ layer, whereas the rest of the film consists of the perovskite phase. In much the same way as it was shown for $RMnO_3$ phases[9] it can be expected that the hexagonal polymorph of $EuFeO_3$ forms on the substrate surface, and the top of the film is formed by perovskite polymorph.

It is interesting to note that lattice spacings of $YbFeO_3$ coincide nearly exactly with those reported for nanopowders except for unit cell symmetry. The centrosymmetric structure of metastable $YAlO_3$-type (space group $P6_3/mmc$) was proposed for nanopowders,[7] but we have found that a set of the observed off-plane reflections for $RFeO_3$ films is not compatible with the $P6_3/mmc$ space group and should be described using $P6_3cm$ with the structure of $LuMnO_3$-type. A direct consequence of the appearance of such a noncentrosymmetric structure is the possibility of ferroelectricity with spontaneous polarization along the hexagonal *c*-axis. It should be mentioned that the optical second harmonic generation was detected in the hexagonal $LuFeO_3$ film on (111) $ZrO_2(Y_2O_3)$ at the room temperature which is a probe for the ferroelectric ordering.[11] A detailed description of the effect will be published elsewhere.

Also, if we trace the *c*/*a* ratio ($c/a\sqrt{3}$ for $P6_3/mmc$) as a formal function of the Goldschmidt tolerance factor for known hexagonal phases of the discussed types (metastable $YAlO_3$ and $LuMnO_3$, see Figure 5), we see that $P6_3/mmc$ was observed only for $t > 0.88$. Our

---

[11] Fiebig, M.; Lottermoser, Th.; Fröhlich, D.; Goltsev, A. V.; Pisarev, R. V. *Nature* **2002**, *419*, 818.

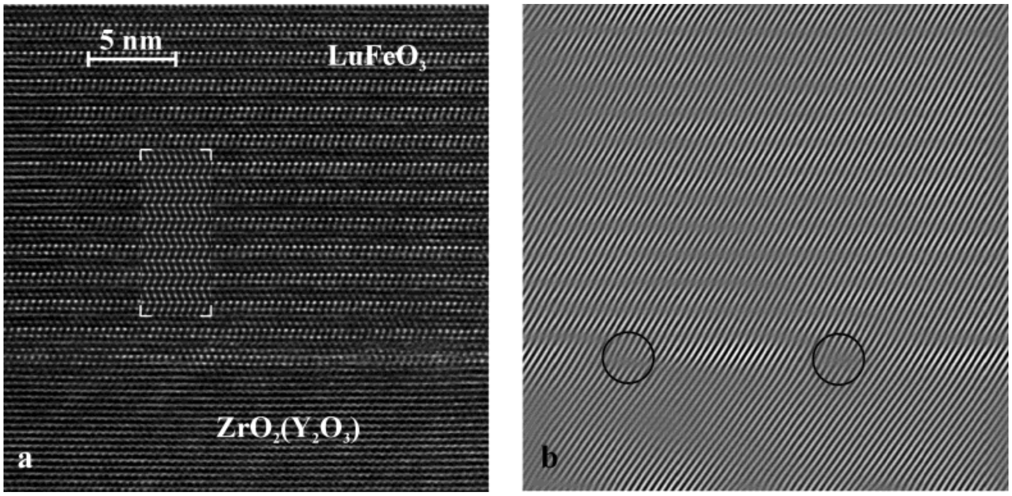

Figure 9. [1$\bar{1}$0] Zone high-resolution image of $LuFeO_3/ZrO_2(Y_2O_3)$ (a) and Fourier-filtered image (b). The inset demonstrates the simulation of HREM image with MacTempas PPC software.

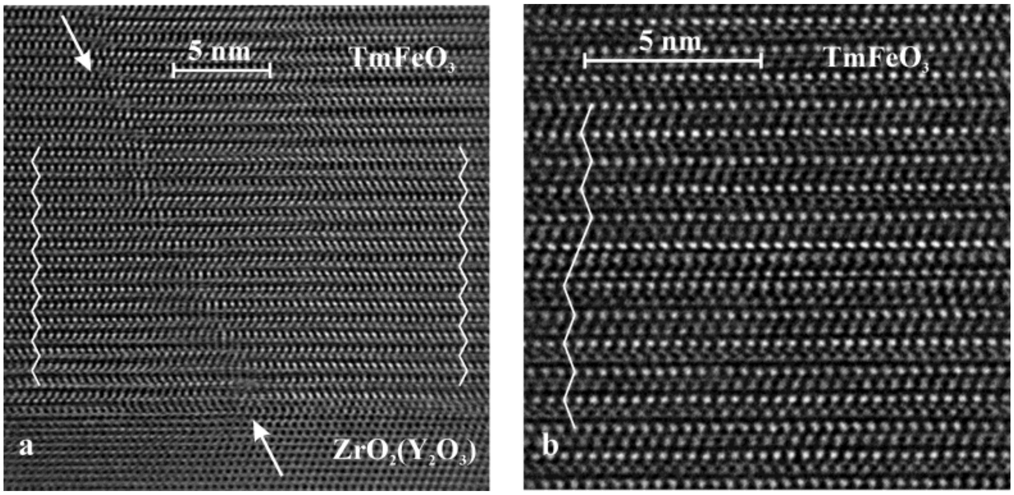

Figure 10. (a) Generation of the antiphase boundary by the substrate step; (b) stacking fault.

experimental points for $RFeO_3$ are evidently in the $P6_3cm$ area (Figure 6).

The epitaxy of the films grown is evident from HREM observations of $TmFeO_3$ and $LuFeO_3$ films. HREM images and ED patterns (Figure 7) were obtained from cross section along the [1$\bar{1}$0] zone of the $ZrO_2(Y_2O_3)$ substrate. ED simulation was performed by MacTempas PPC software using the atomic coordinates for $LuMnO_3$ together with unit cell parameters determined herein (atomic coordinates used are summarized in Table 2). This structure type and domain orientations are consistent with a $LuMnO_3$-type hexagonal structure. No significant quantities of secondary orientations or secondary phases are visible on low-resolution images. The block structure persists, but is much less pronounced than in manganite films[9] (Figure 8).

Misfit dislocations are found (Figure 9) with the spacing not higher than that calculated from film−substrate lattice mismatch, so the films are completely relaxed (the expected density of the misfit dislocations for unstrained film is 60−75 μm^{-1}).

Domain boundaries are apparently extended antiphase boundaries generated by substrate steps (1 ML step giving rise to the antiphase boundary is shown in Figure 10a) and they also can be annihilated on stacking faults such as that shown in Figure 10b. Ferroelectric domains become unobservable in the [1$\bar{1}$0] zone.

As no bulk data are available, we cannot estimate the polymorph stabilization energy as was done for manganites using the linear extrapolation of the bulk $RMnO_3$ formation energy dependencies vs ionic radius for both perovskite and hexagonal polymorphs.[12] But, the estimation can be done regarding the simplified model of the epitaxial stabilization.[13] The contribution of the surface energy is inversely dependent on the layer thickness, and the stabilizing effect can be observed only for the films of limited thickness. For $EuFeO_3$ the thickness of the stabilized layer drops drastically; respectively the energy difference between hexagonal and perovskite phases should be of the order of 10 kJ/mol (typical maximum gain of the free energy by the epitaxial stabilization). Next, the energy difference between polymorphs diminishes along the rare earth element series toward $LuFeO_3$ as the thickness of the stabilized

---

(12) Bosak, A. A.; Kamenev, A. A.; Graboy, I. E.; Antonov, S. V.; Gorbenko, O. Yu.; Kaul, A. R.; Dubourdieu, C.; Senateur, J.-P.; Svechnikov, V. L.; Zandbergen, H. W.; Holländer, B. *Thin Solid Films* **2001**, *400*, 149.

(13) Gorbenko, O. Yu.; Kaul, A. R.; Graboy, I. E.; Samoilenkov, S. V. *Chem. Mater.* **2002**, *14*, 4026.

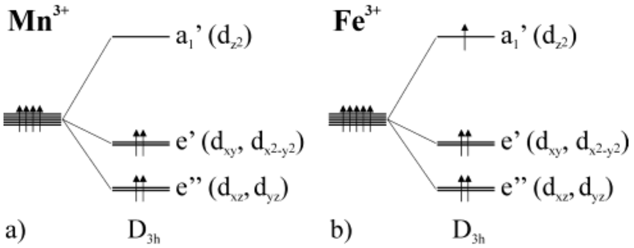

Figure 11. Electron configuration of Mn^{3+} (a) and Fe^{3+} (b) in the trigonal bipyramidal coordination.

layer of the hexagonal phase increases in the same direction.

Compared to that of $RMnO_3$, the unit cell of hexagonal ferrites is axially elongated (Figure 6). This fact can be explained by taking into account the electron configuration of Mn^{3+} (d^4) and Fe^{3+} (d^5) in trigonal bipyramidal coordination (Figure 11).

The highest occupied orbital in the case of Fe^{3+} is z^2 orbital and the axial Fe−O distance should increase because of the repulsion between the electron and oxygen-anion ligands along the *c* axis. The empty z^2 orbital of Mn^{3+} is in agreement with the shorter Mn−O distances along *c* axis than in the *ab* plane. It should be noted that, in contrast to $RMnO_3$ perovskites, no Jahn−Teller distortion takes place in trigonal bipyramidal coordination of Mn^{3+} in the hexagonal $RMnO_3$.[14]

The difference in the electron configuration should contribute to the strain relaxation of the hexagonal $RMnO_3$ and $RFeO_3$ films. In the latter case the relaxation is more rapid with the increase of the film thickness. In fact, only the very thin layer of the hexagonal $EuFeO_3$ is strained, the thicker hexagonal $RFeO_3$ films are already relaxed. In contrast, the manganite films of the same thickness are still epitaxially strained.[15] The strain implies the in-plane stretching of the film structure and respectively the axial contraction both for the ferrites and for the manganites. Whereas in-plane effects are similar for both ions (Fe^{3+} and Mn^{3+}) the axial contraction is much more difficult if the z^2 orbital is occupied as compared to the case of the empty z^2 orbital. Respectively, hexagonal $RFeO_3$ resists the epitaxial deformation more hardly and relaxes more easily.

Conclusion

We have succeeded in the preparation of epitaxial films of hexagonal $RFeO_3$ (R = Eu−Lu) by low-pressure MOCVD. These phases can be formed with the hexagonal structure (instead of the stable perovskite one) because of epitaxial stabilization of the phases on the oxide substrate with fluorite structure of the proper orientation (111). The stabilization effect is valid only for restricted thickness of the film. The assignment of the structure of the hexagonal $RFeO_3$ to a ferroelectric group makes the new material a possible candidate for the ferroelectric memory applications proposed for the hexagonal $RMnO_3$.[16] In addition, because of the high magnetic spin of Fe^{3+}, the magnetic properties of the new material, in particular a possible magnetoelectric effect,[17] deserve further investigation.

Acknowledgment. This work was partly supported by RFBR (02-03-33258), VW Foundation (I/77821), NWO Programme, and INTAS (01-2008) project.

CM0353660

---

(14) Van Aken, B. B.; Meetsma, A.; Palstra, T. *Acta Crystallogr.* **2001**, *E57*, i38.

(15) Bosak, A. A.; Gorbenko, O. Yu.; Kaul, A. R.; Graboy, I. E.; Dubourdieu, C.; Senateur, J. P.; Zandbergen, H. W. *J. Magn. Magn. Mater.* **2000**, *211*, 61.

(16) Fujimura, N.; Ishida, T.; Yoshimura, T.; Ito, T. *Appl. Phys. Lett.* **1996**, *69*, 1011.

(17) Wang, J.; Neaton, J. B.; Zheng, H.; Nagarajan, V.; Ogale, S. B.; Liu, B.; Viehland, D.; Vaithyanathan, V.; Schlom, D. G.; Waghmare, U. V.; Spaldin, N. A.; Rabe, K. M.; Wuttig, M.; Ramesh, R. *Science* **2003**, *299*, 1719.